Electronic Supplementary Material (ESI) for Physical Chemistry Chemical Physics.

Supporting Information

Balancing Dipolar and Exchange Coupling in Biradicals to Maximize Cross Effect Dynamic Nuclear Polarization

Asif Equbal,[†] Kan Tagami,[†] and Songi Han[*,†,‡]

†*Department of Chemistry and Biochemistry, University of California, Santa Barbara, Santa Barbara, California 93106, United States.*

‡*Department of Chemical Engineering, University of California, Santa Barbara, Santa Barbara, California 93106, United States.*

E-mail: songi@chem.ucsb.edu

Contents

A. Numerical simulation

The Cross-Effect MAS-DNP simulations were performed using Spin-Evolution software package, for a 3-spin system, including 2 electron spins ($e_1 - e_2$) and a nuclear spin (^{1}H). The calculations were rotor-synchronized and performed in Liouville space to incorporate for the effects of e and ^{1}H spin relaxation- which are crucial in all the DNP mechanisms. The DNP enhancements under μw irradiation was measured with respect to the thermal Boltzmann polarization of proton under static. Powder averaging was performed using 50 (α, β) angles, unless mentioned otherwise. Notably, numerical results with larger number of orientations showed the same trend. The simulations were performed for two classes of radicals- (1) bis-nitroxide, with e_1 and e_2 representing nitroxide radical in the $e_1 - e_2 - ^1$H spin system, and (2) tethered narrow and broad-line radicals, with e_1 and e_2 representing narrow and broad-line radical, respectively, in the $e_1 - e_2 - ^1$H spin system. The principal axis components of the g-tensors of the electrons were taken as: Narrow-line: gx=2.0034, gy=2.0031, gz=2.0027, and Broad (nitroxide): gx=2.0098, gy=2.0064, gz=2.0024. Unless mentioned otherwise, the spin parameters used for the calculations were as follows: the g-tensor of e_2 was related to e_1 by the Euler angles sets, (107,90,124) and (90,90,-45) in bis-nitroxide and mixed radical, respectively, using $z-y-z$ convention. In both types of radicals, the relative $e_1 - e_2$ dipolar tensor orientation was given by the Euler angles (0,75,0). The choice of the above orientations are only a rough estimate (taken from earlier simulations) since the exact orientations of the spin tensors are not known. The orientation of the $e_1 -^1 H$ and $e_2 -^1 H$ hyperfine couplings were randomly chosen to be (0,45,270) and (0, 10, 90), respectively. The $e_1 -^1 H$, and $e_2 -^1 H$ couplings were taken to be 2 MHz ($r_{e_1-^1H}$=3.40 $\mathring{A}$), and 0.043 MHz ($r_{e_2-^1H}$=12.06 $\mathring{A}$), respectively, for both the radicals. The nuclear spin-lattice relaxation rate, T_{1H}, was always set to 4 s. Unless mentioned otherwise, T_{1e} of the two electron spins was set to 10 times the rotor period. The μw irradiation frequency was set to the optimal DNP conditions at each magnetic field. Polarization of all the spins were measured with respect to the Boltzmann polarization of protons under static conditions at 100 K. Therefore,

the ^{1}H-ϵ_{DNP} also includes the nuclear depolarization factor in all our calculations.

B. Results

Nuclear spin depolarization under MAS

J and Dipolar interference leads to nuclear spin depolarization, which is defined as the relative NMR signal intensity under MAS over static conditions in the absence of μw irradiation due to CE mechanisms, i.e. ^1H-ϵ_{depo}=^1H-$\epsilon_{spin,no\ \mu w}$/$^1H$-$\epsilon_{static,no\ \mu w}$. As seen in Fig. S1b, ^1H-ϵ_{depo} decreases under the conditions $0.2 \leq$ J/D ≤ 1. The similar comparison is done for mixed radical system in Figure S2. The 2D depolarization profiles for the two radical systems are shown in Fig. S3.

Polarization difference, ΔP_e vs. J/D

In Fig. S4, the ^1H DNP enhancement and electron spins polarization difference (ΔP_e) are plotted as a function of J/D, using bis-nitroxide. The D was fixed to 36 MHz. All the parameters are same as used in Fig. 1. Clearly, the lower DNP enhancements at the interference conditions are a manifestation of reduced ΔP_e; a result of non-adiabatic e-e rotor events.

Magnetic field dependence

In Fig. S5, the ^1H DNP enhancement is plotted as a function of J+D and magnetic field for 10 kHz and 20 kHz spinning frequencies. The ratio J/D was fixed to 2.5. All the parameters are same as used in Fig. S3. Simulations show that J+D roughly around 1/10 of the Larmor frequency is optimum for maximum DNP enhancement. Larger J+D that leads to splitting of the EPR line at the isotropic g. This reduces the DNP enhancement.

Spinning frequency dependence

In Fig. S6, the ^1H DNP enhancement is plotted as a function of J+D and spinning frequency under 18.8 T field conditions. The ratio J/D was fixed to 1.5 and 2.5 in subplots a and b. All the parameters are same as used in Fig S3. Simulations show that optimum J+D and J/D lead to large DNP enhancement across a wide range of spinning frequency. Optimum coupling parameters leads to larger adiabaticity even at when the energy crossing rates are fast as discussed in the main text.

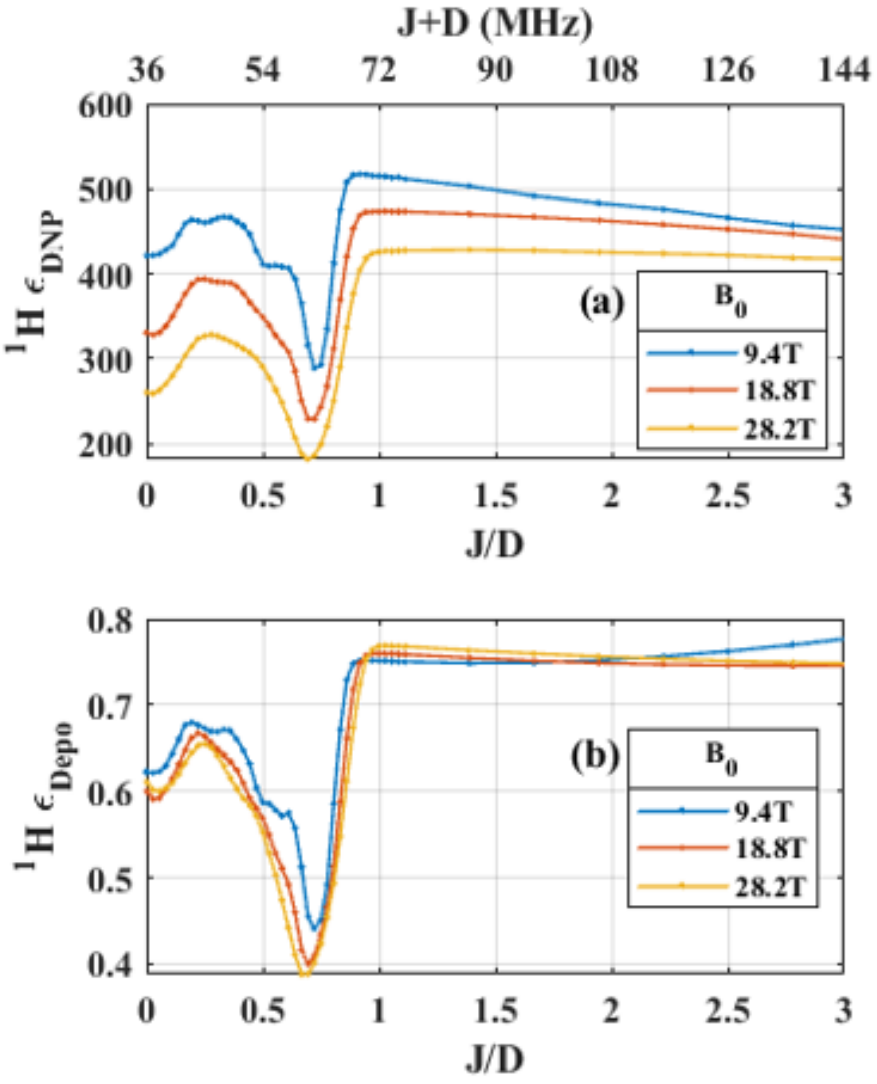

Figure S1: **Numerically simulated J/D profiles for bis-nitroxide.** (a) ^{1}H enhancement vs. J/D (and J+D) for three different magnetic fields using 0.8 MHz μw B_1 at 10 kHz spinning. (b) Corresponding ^{1}H depolarization profiles. The simulations were performed using $e_1 - e_2 - ^1$H spin system, taking the g-tensors of the tethered nitroxide (e_1)-nitroxide (e_2) radical with perpendicular g-tensor orientations. D was fixed to 36 MHz. T_{1e} of the two electron spins was set to 10 times the spinning at 10 kHz.

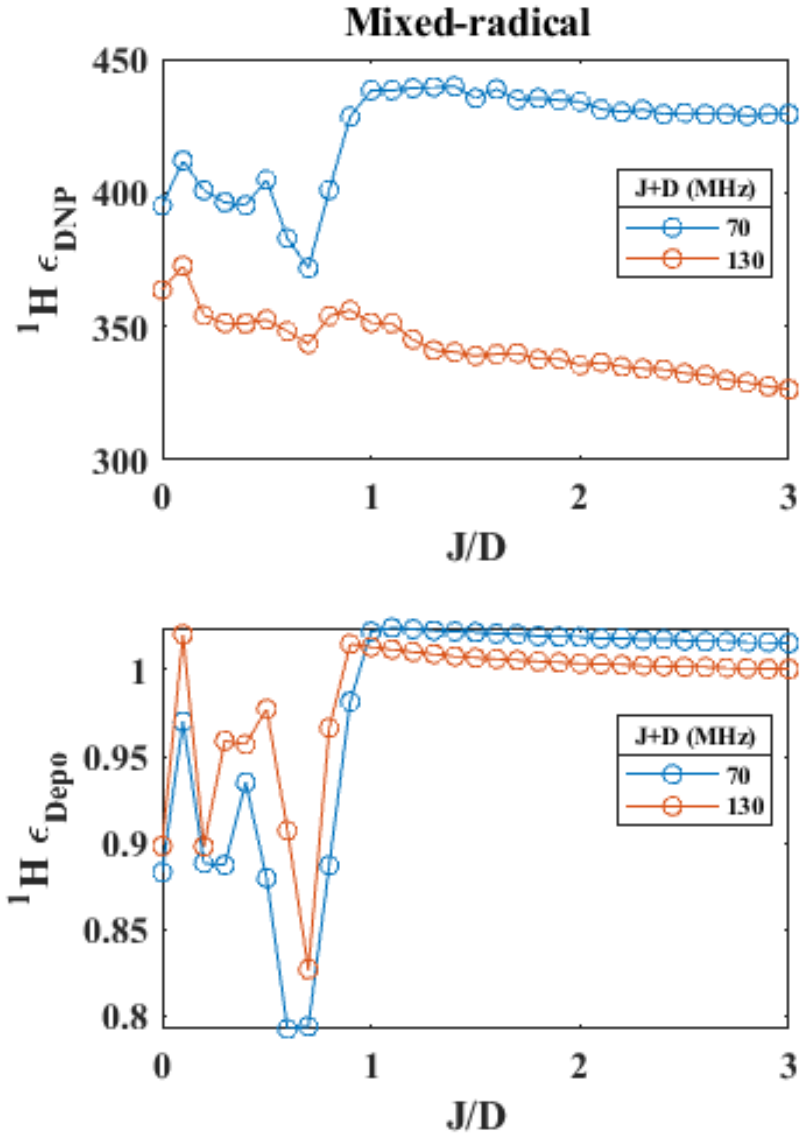

Figure S2: **Numerically simulated J/D profiles for mixed-radicals.** (a) ^{1}H enhancement vs. J/D for two different J+D using 0.8 MHz μw B_1 at 20 kHz spinning. (b) Corresponding ^{1}H depolarization profiles. The simulations were performed using $e_1 - e_2 - ^1$H spin system, mimicking mixed-radical. T_{1e} of the two electron spins was set to 10 times the rotor period.

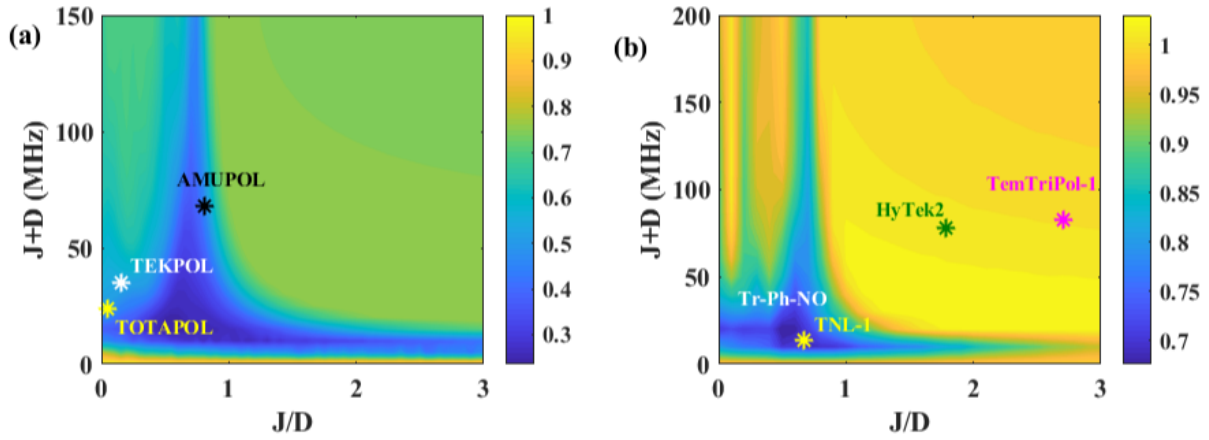

Figure S3: **Numerically simulated 2D nuclear spin depolarization profile.** ^{1}H depolarization vs. J/D and J+D for (a) bis-nitroxide (b) mixed narrow and broad-line radicals. The simulations were done for the same system as in Fig. 2a and 2c of the main text, but under μw off conditions.

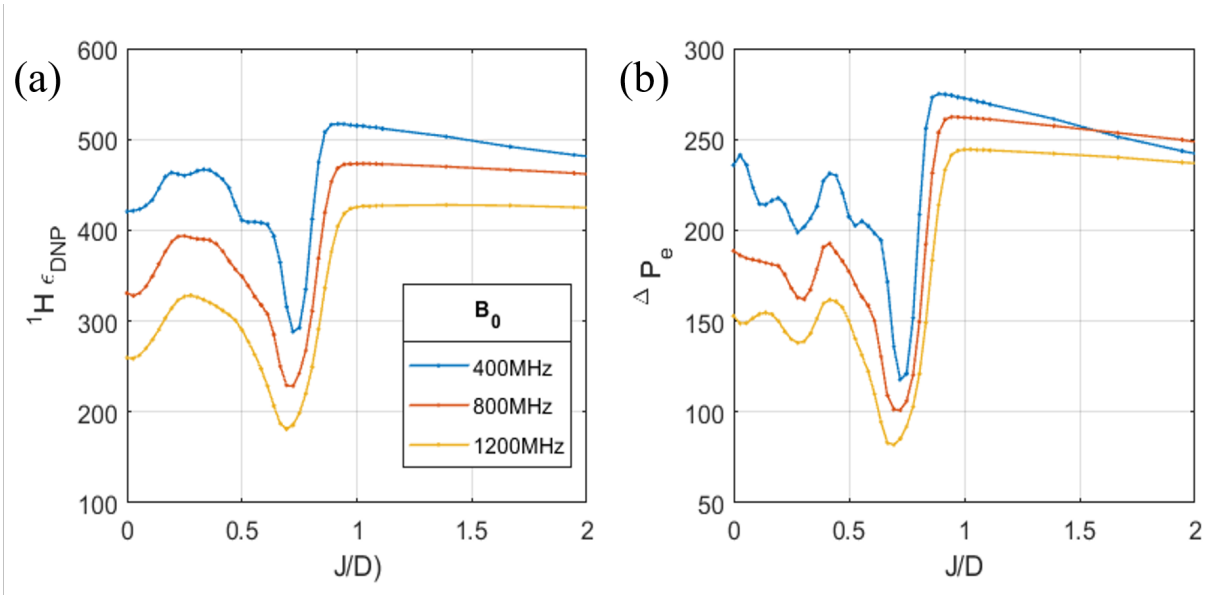

Figure S4: ΔP_e **vs. J/D.** Numerically simulated, (a) nuclear Polarization enhancement and (b) corresponding electrons polarization difference, ΔP_e vs. J/D using bis-nitroxide at three different B_0. All the parameters are same as in Fig. 1 of the main text. ν_r=10 kHz, μw B_1=0.8 MHz and T_{1e}=10τ_r=1 ms.

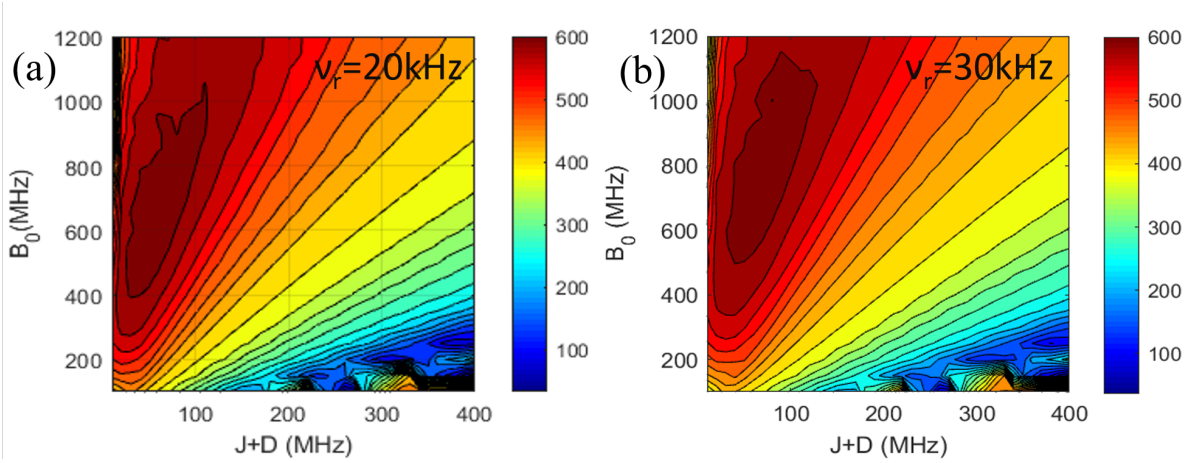

Figure S5: **Magnetic field dependence for mixed radical.** Numerically simulated ^{1}H DNP enhancement as a function of magnetic field (as proton Larmor frequency) and the sum, J+D, at two different MAS frequencies: (a) 20 kHz and (b) 30 kHz. Following parameters were used: μw B_1=1.8 MHz and T_{1e_1}=2*T_{1e_2}=10τ_r. J/D=2.5.

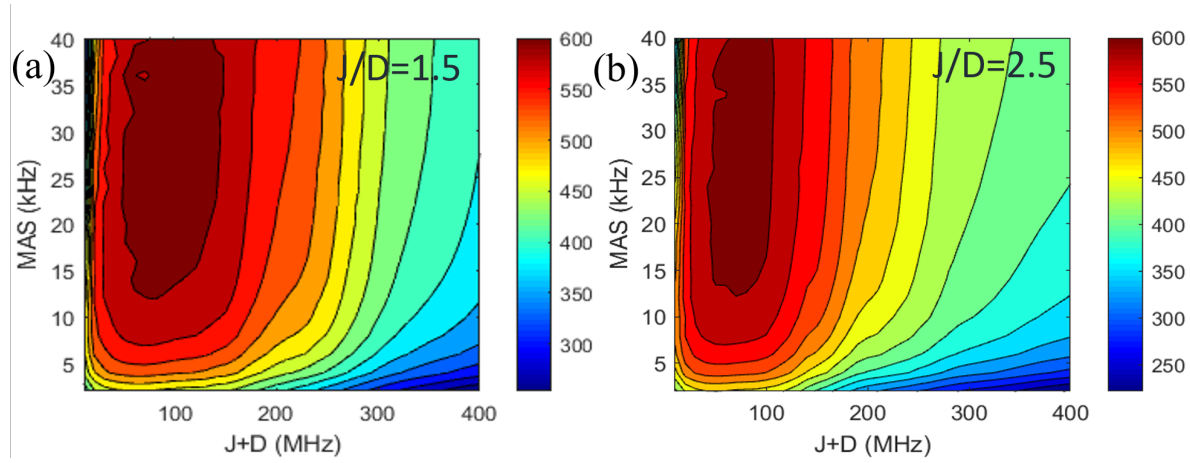

Figure S6: **MAS Frequency dependence for mixed radical** Numerically simulated ^{1}H DNP enhancement as a function of spinning frequency and the sum, J+D, for two different J/D: (a) 1.5 and (b) 2.5. Following parameters were used: B_0= 18.8 T, μw B_1=1.8 MHz and T_{1e_1}=2*T_{1e_2}=0.5 ms.

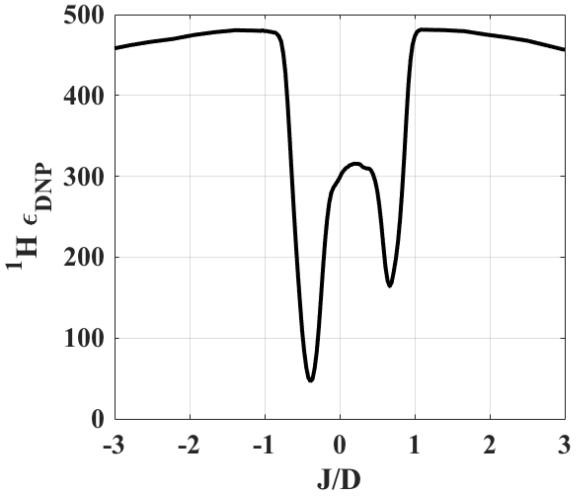

Figure S7: **Numerically simulated J/D profiles for bis-nitroxide.** (a) ^{1}H enhancement vs. J/D using 0.8 MHz μw B_1 at 20 kHz spinning and all other spin parameters same as in Figure 1 of the manuscript. The profile shows that interference between J and D for the positive and negative values of J/D.